Electronic Supplementary Material (ESI) for Journal of Materials Chemistry C.

Supporting Information

Ag migration mechanism in heated metal/ceramic nano-multilayers: interplay between stress-relaxation and oxygen-mediated mass transport.

Mirco Chiodi[1], Claudia Cancellieri[1], Frank Moszner[1], Mariusz Andrzejczuk[2], Jolanta Janczak-Rusch[1], Lars P.H. Jeurgens[1]

[1] Empa, Swiss Federal Laboratories for Materials Science and Technology, Laboratory for Joining and Interface Technology, Überlandstrasse 129, 8600 Dübendorf, Switzerland.

[2] Warsaw University of Technology, Faculty of Materials Science and Engineering, Wołoska 141, 02-507 Warsaw, Poland

Thermal treatments of NMLs in vacuum, as well as of a thick Ag layer sandwiched between thin AlN barriers.

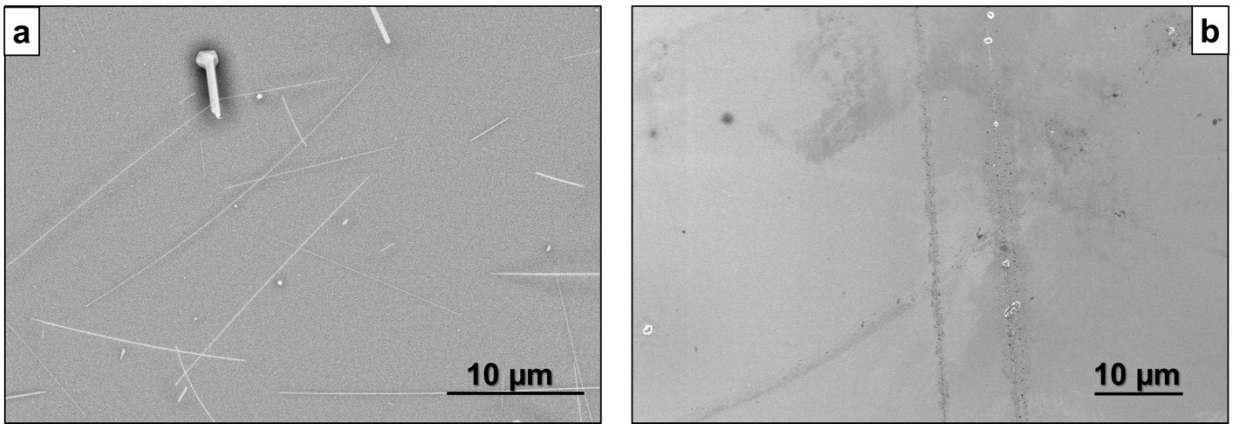

Figure S1 ***(a)*** *SEM micrograph of the Ag/AlN NML surface after heating at 420°C in UHV.* ***(b)*** *SEM micrograph of a 200-nm thick Ag layer sandwiched between two AlN barriers (10 nm thick) after heating at 420°C in air. In both cases, no extensive formation of Ag particles on the surface is observed.*

The Ag/AlN NML under study (on the identical α-$Al_2O_3(1\bar{1}02)$ substrate) was heated up to 420°C under UHV conditions (instead of in air at atmospheric pressure): see Fig. S1a. Furthermore, an identical thermal treatment was performed in air on a thick Ag layer (200 nm), which was sandwiched between two 10 nm thick AlN barriers, on the α-$Al_2O_3(1\bar{1}02)$ substrate: see Fig. S1b. In both this cases, **no** extensive Ag migration from the confined Ag nanolayers to the outer surface was observed (Figure S1).

Superlattice XRD spectrum calculation

XRD analysis of artificial superlattices (SL) constituted of two different constituents (*here:* Ag and AlN) typically shows additional diffraction peaks around the main Bragg reflection of the pure constituents related to the imposed periodicity, which intensities are modulated by the structure factor of the building period (*here:* the Ag/AlN bilayer unit). Indeed, such so-called "satellite peaks", as originating from the constructive interference between [111]-oriented Ag and [001]-oriented AlN grains, are observed in the t2t range of 32 - 42°. Figure S2 shows a comparison of the measured and a calculated XRD diffractogram for the as-deposited state from 2θ = 30 - 45°.

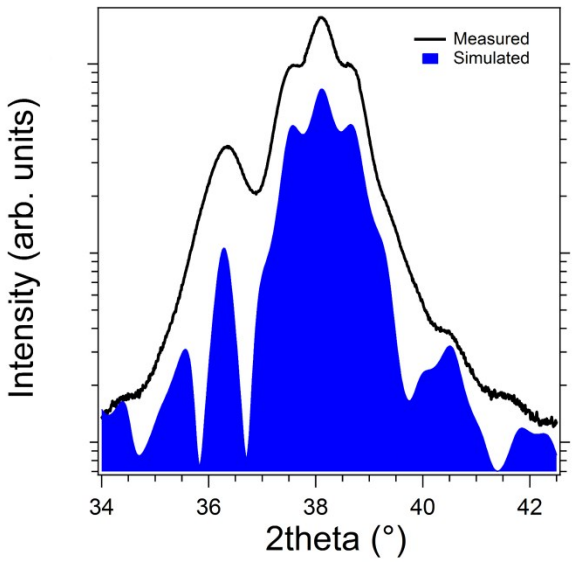

Figure S2 - Comparison of the measured (black) and calculated (blue) diffractograms

The theoretical diffractogram was calculated on the basis of a kinematic formalism to obtain the diffracted intensity from the mean structure factor of the constituent blocks[65] using the following basic model input parameters: unit-cell dimensions of the constituents, the number of layers of each constituent per block (N_{Ag} and N_{AlN}) and the total number of SL periods (M). A degradation of crystal coherence within the SL configuration affects the shape of the resulting XRD patterns, especially towards high diffraction angles[66]. To account for such disorder, the

following additional model input parameters were introduced: i.e. the *intralayer* disorder, σ, which described the effect of random displacements (disorder) *within* the individual layers and the *interlayer* disorder, Σ, which accounts for random displacements (disorder) at the *interfaces* between successive layers. Both displacements were assumed to have zero average and a Gaussian distribution. The introduction of σ and Σ was necessary in order to reproduce the broadening of the satellite peaks. The presence of these two parameters is compatible with the observed roughening in the NML (see cross-sectional TEM in Fig.1c).

The best model description of the experimental diffractograms of the as-deposited NML in the t2t range of 30 - 45° were obtained for $N_{\mathrm{Ag}} = 25$, $N_{\mathrm{AlN}} = 38$, $d_{Ag}^{111} = 0.236$ nm, $d_{AlN}^{001} = 0.234$ nm, σ = 0.1 Å and Σ = 0.4 Å. The fitted total bilayer period of $(d_{Ag}^{111} \times N_{\mathrm{Ag}} + d_{AlN}^{001} \times N_{\mathrm{AlN}})$ of 13.5 nm is in very good agreement with the nominal experimentally obtained bilayer thickness of 15 nm.

Real-time XRD measurement and stress evaluation

The stress evolution during heating and cooling was investigated using the Uniform Stress Deformation Model (USDM), which is an extension of the Williamson-Hall model for an anisotropic strain case.

In fact, accounting for the differences in the Young's modulus along different crystallographic directions (Y_{hkl}) in the fcc Ag metal, it holds that

$$\beta_{hkl}\cos\theta_{hkl} = \frac{K\lambda}{D} + \frac{4\sigma\sin\theta_{hkl}}{Y_{hkl}}, \quad (1)$$

where β_{hkl} is the (instrumentally corrected) FWHM of a given *hkl* reflection; θ is the corresponding Bragg angle; K is a numeric constant related to the crystallite shape (*here:* 0.94),: λ is the X-ray wavelength; D is the crystallite size; σ is the average stress and Y_{hkl} represents the Young modulus along the analyzed crystallographic direction. The first term in Eq. (1) describes the broadening contribution due to the limited coherency length of the crystalline domain (according to the so-called Sherrer formula), while the second term describes the strain-induced broadening contribution. Considering two identical reflections of different order (i.e. Ag(111) and Ag(222)), it follows that:

$$\beta_{111}\cos\theta_{111} - \frac{4\sigma\sin\theta_{111}}{Y_{111}} = \beta_{222}\cos\theta_{222} - \frac{4\sigma\sin\theta_{222}}{Y_{111}} = \frac{K\lambda}{D}, \quad (2a)$$

which gives

$$\frac{\sigma}{Y_{111}} = \frac{\beta_{111}\cos\theta_{111} - \beta_{222}\cos\theta_{222}}{4(\sin\theta_{111}\sin\theta_{222})} = \varepsilon_{111}, \quad (2b)$$

where ε_{111} is the microstrain along the <111> direction. The calculated Young's modulus along the <111> direction in Ag metal equals 120.1 GPa, which allows for an estimation of the residual stress as a function of temperature as presented in the main text (see Fig. 6).

References

(65) Clemens, B. M.; Gay, J. G., *Phys. Rev. B* **1987**, *35*, 9337.

(66) Abadias, G.; Tse, Y. Y.; Michel, A.; Jaouen, C.; Jaouen, M., *Thin Solid Films* **2003**, *433*, 166–173.